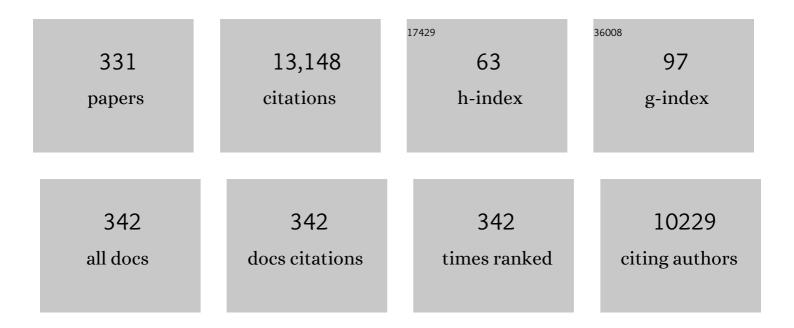
List of Publications by Year in descending order

Source: https://exaly.com/author-pdf/5401217/publications.pdf Version: 2024-02-01



#	Article	IF	CITATIONS
1	Computational Prediction for Singlet- and Triplet-Transition Energies of Charge-Transfer Compounds. Journal of Chemical Theory and Computation, 2013, 9, 3872-3877.	2.3	312
2	Methane-to-Methanol Conversion by First-Row Transition-Metal Oxide Ions:Â ScO+, TiO+, VO+, CrO+, MnO+, FeO+, CoO+, NiO+, and CuO+. Journal of the American Chemical Society, 2000, 122, 12317-12326.	6.6	262
3	Catalytic transformation of dinitrogen into ammonia and hydrazine by iron-dinitrogen complexes bearing pincer ligand. Nature Communications, 2016, 7, 12181.	5.8	244
4	Orbital Views of the Electron Transport in Molecular Devices. Journal of the American Chemical Society, 2008, 130, 9406-9413.	6.6	223
5	Catalytic Reduction of Dinitrogen to Ammonia by Use of Molybdenum–Nitride Complexes Bearing a Tridentate Triphosphine as Catalysts. Journal of the American Chemical Society, 2015, 137, 5666-5669.	6.6	215
6	Catalytic Formation of Ammonia from Molecular Dinitrogen by Use of Dinitrogen-Bridged Dimolybdenum–Dinitrogen Complexes Bearing PNP-Pincer Ligands: Remarkable Effect of Substituent at PNP-Pincer Ligand. Journal of the American Chemical Society, 2014, 136, 9719-9731.	6.6	202
7	Interplay between Theory and Experiment for Ammonia Synthesis Catalyzed by Transition Metal Complexes. Accounts of Chemical Research, 2016, 49, 987-995.	7.6	200
8	Remarkable catalytic activity of dinitrogen-bridged dimolybdenum complexes bearing NHC-based PCP-pincer ligands toward nitrogen fixation. Nature Communications, 2017, 8, 14874.	5.8	198
9	Intrinsic reaction coordinate analysis of the conversion of methane to methanol by an iron–oxo species: A study of crossing seams of potential energy surfaces. Journal of Chemical Physics, 1999, 111, 538-545.	1.2	191
10	Direct Transformation of Molecular Dinitrogen into Ammonia Catalyzed by Cobalt Dinitrogen Complexes Bearing Anionic PNP Pincer Ligands. Angewandte Chemie - International Edition, 2016, 55, 14291-14295.	7.2	184
11	Methaneâ~'Methanol Conversion by MnO+, FeO+, and CoO+:Â A Theoretical Study of Catalytic Selectivity. Journal of the American Chemical Society, 1998, 120, 564-572.	6.6	164
12	A light-induced spin crossover actuated single-chain magnet. Nature Communications, 2013, 4, .	5.8	162
13	Unique behaviour of dinitrogen-bridged dimolybdenum complexes bearing pincer ligand towards catalytic formation of ammonia. Nature Communications, 2014, 5, 3737.	5.8	162
14	Catalytic Nitrogen Fixation via Direct Cleavage of Nitrogen–Nitrogen Triple Bond of Molecular Dinitrogen under Ambient Reaction Conditions. Bulletin of the Chemical Society of Japan, 2017, 90, 1111-1118.	2.0	156
15	Molybdenum-Catalyzed Transformation of Molecular Dinitrogen into Silylamine: Experimental and DFT Study on the Remarkable Role of Ferrocenyldiphosphine Ligands. Journal of the American Chemical Society, 2011, 133, 3498-3506.	6.6	148
16	Methane selective oxidation to methanol by metal-exchanged zeolites: a review of active sites and their reactivity. Catalysis Science and Technology, 2019, 9, 1744-1768.	2.1	148
17	Conversion of Methane to Methanol at the Mononuclear and Dinuclear Copper Sites of Particulate Methane Monooxygenase (pMMO):Â A DFT and QM/MM Study. Journal of the American Chemical Society, 2006, 128, 9873-9881.	6.6	146
18	Direct Conversion of Methane to Methanol by Metal-Exchanged ZSM-5 Zeolite (Metal = Fe, Co, Ni, Cu). ACS Catalysis, 2016, 6, 8321-8331.	5.5	141

#	Article	IF	CITATIONS
19	Direct Methaneâ^'Methanol and Benzeneâ^'Phenol Conversions on Feâ^'ZSM-5 Zeolite:  Theoretical Predictions on the Reaction Pathways and Energetics. Journal of Physical Chemistry B, 2000, 104, 734-740.	1.2	139
20	Sulfurâ^'Gold Orbital Interactions which Determine the Structure of Alkanethiolate/Au(111) Self-Assembled Monolayer Systems. Journal of Physical Chemistry B, 2002, 106, 12727-12736.	1.2	135
21	An Orbital Rule for Electron Transport in Molecules. Accounts of Chemical Research, 2012, 45, 1612-1621.	7.6	135
22	Ruthenium atalyzed Selective and Efficient Oxygenation of Hydrocarbons with Water as an Oxygen Source. Angewandte Chemie - International Edition, 2008, 47, 5772-5776.	7.2	133
23	Roles of Zeolite Confinement and Cu–O–Cu Angle on the Direct Conversion of Methane to Methanol by [Cu ₂ (μ-O)] ²⁺ -Exchanged AEI, CHA, AFX, and MFI Zeolites. ACS Catalysis, 2017, 7, 3741-3751.	5.5	129
24	Molecular Understanding of the Adhesive Force between a Metal Oxide Surface and an Epoxy Resin. Journal of Physical Chemistry C, 2011, 115, 11701-11708.	1.5	126
25	Catalytic Mechanism of Dopamine β-Monooxygenase Mediated by Cu(III)â^'Oxo. Inorganic Chemistry, 2006, 45, 3034-3041.	1.9	123
26	Theoretical Study of Donorâ^'Ï€-Bridgeâ^'Acceptor Unimolecular Electric Rectifier. Journal of Physical Chemistry C, 2007, 111, 11699-11705.	1.5	121
27	Theoretical Study of the Direct Synthesis of H ₂ O ₂ on Pd and Pd/Au Surfaces. Journal of Physical Chemistry C, 2008, 112, 19501-19505.	1.5	121
28	Abstraction of the Hydrogen Atom of Methane by Ironâ^'Oxo Species:Â The Concerted Reaction Path Is Energetically More Favorable. Organometallics, 1998, 17, 2825-2831.	1.1	119
29	Iron-catalysed transformation of molecular dinitrogen into silylamine under ambient conditions. Nature Communications, 2012, 3, 1254.	5.8	118
30	Reaction Paths for the Conversion of Methane to Methanol Catalyzed by FeO ⁺ . Chemistry - A European Journal, 1997, 3, 1160-1169.	1.7	114
31	Nonradical Mechanism for Methane Hydroxylation by Iron-Oxo Complexes. Accounts of Chemical Research, 2006, 39, 375-382.	7.6	111
32	Cleavage and Formation of Molecular Dinitrogen in a Single System Assisted by Molybdenum Complexes Bearing Ferrocenyldiphosphine. Angewandte Chemie - International Edition, 2014, 53, 11488-11492.	7.2	111
33	Molecular motor-driven abrupt anisotropic shape change in a single crystal of a Ni complex. Nature Chemistry, 2014, 6, 1079-1083.	6.6	111
34	Catalytic Reduction of Molecular Dinitrogen to Ammonia and Hydrazine Using Vanadium Complexes. Angewandte Chemie - International Edition, 2018, 57, 9064-9068.	7.2	109
35	The role of orbital interactions in determining ferromagnetic coupling in organic molecular assemblies. Journal of the American Chemical Society, 1995, 117, 6921-6926.	6.6	107
36	A ferromagnetically coupled Fe42 cyanide-bridged nanocage. Nature Communications, 2015, 6, 5955.	5.8	104

#	Article	IF	CITATIONS
37	Methane Partial Oxidation over [Cu ₂ (μ-O)] ²⁺ and [Cu ₃ (μ-O) ₃] ²⁺ Active Species in Large-Pore Zeolites. ACS Catalysis, 2018, 8, 1500-1509.	5.5	104
38	Comparison of the Reactivity of Bis(μ-oxo)Cu ^{II} Cu ^{III} and Cu ^{III} Cu ^{III} Species to Methane. Inorganic Chemistry, 2009, 48, 838-845.	1.9	102
39	Nitrogen fixation catalyzed by ferrocene-substituted dinitrogen-bridged dimolybdenum–dinitrogen complexes: unique behavior of ferrocene moiety as redox active site. Chemical Science, 2015, 6, 3940-3951.	3.7	100
40	Dioxygen Cleavage and Methane Activation on Diiron Enzyme Models:Â A Theoretical Study. Journal of the American Chemical Society, 1997, 119, 12311-12321.	6.6	97
41	A spin–orbit coupling study on the spin inversion processes in the direct methane-to-methanol conversion by FeO+. Journal of Chemical Physics, 2003, 118, 5872-5879.	1.2	97
42	Orbital Views of Molecular Conductance Perturbed by Anchor Units. Journal of the American Chemical Society, 2011, 133, 5955-5965.	6.6	94
43	Reaction Pathway for the Direct Benzene Hydroxylation by Ironâ^'Oxo Species. Journal of the American Chemical Society, 1999, 121, 147-153.	6.6	91
44	Quantum Transport Effects in Nanosized Graphite Sheets. ChemPhysChem, 2002, 3, 1035-1037.	1.0	90
45	Theoretical Study of the Decomposition and Hydrogenation of H ₂ O ₂ on Pd and Au@Pd Surfaces: Understanding toward High Selectivity of H ₂ O ₂ Synthesis. Journal of Physical Chemistry C, 2011, 115, 7392-7398.	1.5	90
46	Dependence of Single-Molecule Conductance on Molecule Junction Symmetry. Journal of the American Chemical Society, 2011, 133, 11426-11429.	6.6	89
47	Theoretical Revisit of the Direct Synthesis of H ₂ O ₂ on Pd and Au@Pd Surfaces: A Comprehensive Mechanistic Study. Journal of Physical Chemistry C, 2011, 115, 25359-25367.	1.5	89
48	Theoretical Overview of Methane Hydroxylation by Copper–Oxygen Species in Enzymatic and Zeolitic Catalysts. Accounts of Chemical Research, 2018, 51, 2382-2390.	7.6	85
49	Adsorption and Activation of Methane on the (110) Surface of Rutile-type Metal Dioxides. Journal of Physical Chemistry C, 2018, 122, 15359-15381.	1.5	85
50	Computational Exploration of the Catalytic Mechanism of Dopamine β-Monooxygenase: Modeling of Its Mononuclear Copper Active Sites. Inorganic Chemistry, 2005, 44, 4226-4236.	1.9	82
51	Photoswitching of Conductivity through a Diarylperfluorocyclopentene Nanowire. Journal of Physical Chemistry C, 2007, 111, 3517-3521.	1.5	82
52	Cobalt atalyzed Transformation of Molecular Dinitrogen into Silylamine under Ambient Reaction Conditions. Chemistry - A European Journal, 2015, 21, 8905-8909.	1.7	80
53	Specific Enhancement of Catalytic Activity by a Dicopper Core: Selective Hydroxylation of Benzene to Phenol with Hydrogen Peroxide. Angewandte Chemie - International Edition, 2017, 56, 7779-7782.	7.2	77
54	A Lowâ€Spin Ruthenium(IV)–Oxo Complex: Does the Spin State Have an Impact on the Reactivity?. Angewandte Chemie - International Edition, 2010, 49, 8449-8453.	7.2	76

#	Article	IF	CITATIONS
55	Mechanistic Study on the Production of Hydrogen Peroxide in the Anthraquinone Process. European Journal of Organic Chemistry, 2011, 2011, 4113-4120.	1.2	76
56	Theoretical Study of Long-Range Electron Transport in Molecular Junctions. Journal of Physical Chemistry C, 2008, 112, 17408-17415.	1.5	73
57	Homogeneous Photocatalytic Water Oxidation with a Dinuclear Co ^{III} –Pyridylmethylamine Complex. Inorganic Chemistry, 2016, 55, 1154-1164.	1.9	73
58	Electron–phonon coupling in negatively charged acene- and phenanthrene-edge-type hydrocarbon crystals. Journal of Chemical Physics, 2002, 116, 3420-3429.	1.2	72
59	Quantum Chemical Approach to the Mechanism for the Biological Conversion of Tyrosine to Dopaquinone. Journal of the American Chemical Society, 2008, 130, 16890-16897.	6.6	70
60	Two-step concerted mechanism for alkane hydroxylation on the ferryl active site of methane monooxygenase. Journal of Biological Inorganic Chemistry, 1998, 3, 318-324.	1.1	69
61	Assembling an alkyl rotor to access abrupt and reversible crystalline deformation of a cobalt(II) complex. Nature Communications, 2015, 6, 8810.	5.8	69
62	Wire-Length Dependence of the Conductance of Oligo(p-phenylene) Dithiolate Wires:  A Consideration from Molecular Orbitals. Journal of Physical Chemistry A, 2004, 108, 9143-9149.	1.1	66
63	Bistability of Magnetization without Spin-Transition in a High-Spin Cobalt(II) Complex due to Angular Momentum Quenching. Journal of the American Chemical Society, 2009, 131, 4560-4561.	6.6	63
64	Role of Edge Oxygen Atoms on the Adhesive Interaction between Carbon Fiber and Epoxy Resin. Journal of Physical Chemistry C, 2013, 117, 24830-24835.	1.5	60
65	Role of Tyrosine Residue in Methane Activation at the Dicopper Site of Particulate Methane Monooxygenase: A Density Functional Theory Study. Inorganic Chemistry, 2013, 52, 7907-7917.	1.9	58
66	Superior thermoelasticity and shape-memory nanopores in a porous supramolecular organic framework. Nature Communications, 2016, 7, 11564.	5.8	58
67	Molecular Understanding of the Adhesive Force between a Metal Oxide Surface and an Epoxy Resin: Effects of Surface Water. Bulletin of the Chemical Society of Japan, 2012, 85, 672-678.	2.0	57
68	Dioxygen Binding to Dinuclear Iron Centers on Methane Monooxygenase Models. Inorganic Chemistry, 1996, 35, 2409-2410.	1.9	56
69	Formation of an Iron-Oxo Species upon Decomposition of Dinitrogen Oxide on a Model of Fe-ZSM-5 Zeolite. Bulletin of the Chemical Society of Japan, 2000, 73, 29-36.	2.0	56
70	A Theoretical Study of Alcohol Oxidation by Ferrate. Journal of Organic Chemistry, 2001, 66, 4122-4131.	1.7	56
71	Surface Oxygen Atom as a Cooperative Ligand in Pd Nanoparticle Catalysis for Selective Hydration of Nitriles to Amides in Water: Experimental and Theoretical Studies. ACS Catalysis, 2012, 2, 2467-2474.	5.5	56
72	Multiply-fused porphyrins—effects of extended ï€-conjugation on the optical and electrochemical properties. Chemical Communications, 2013, 49, 5939.	2.2	56

#	Article	IF	CITATIONS
73	Direct Transformation of Molecular Dinitrogen into Ammonia Catalyzed by Cobalt Dinitrogen Complexes Bearing Anionic PNP Pincer Ligands. Angewandte Chemie, 2016, 128, 14503-14507.	1.6	56
74	Green's function formalism coupled with Gaussian broadening of discrete states for quantum transport: Application to atomic and molecular wires. Journal of Chemical Physics, 2004, 121, 8050.	1.2	55
75	Conversion of Methane to Methanol on Diiron and Dicopper Enzyme Models of Methane Monooxygenase: A Theoretical Study on a Concerted Reaction Pathway. Bulletin of the Chemical Society of Japan, 2000, 73, 815-827.	2.0	54
76	Potential Linear hain Organic Ferromagnets. Chemistry - A European Journal, 1995, 1, 403-413.	1.7	53
77	Reaction Pathways for the Oxidation of Methanol to Formaldehyde by an Ironâ^'Oxo Species. Journal of Physical Chemistry A, 2000, 104, 9347-9355.	1.1	50
78	Orbital Control of the Conductance Photoswitching in Diarylethene. Journal of Physical Chemistry C, 2009, 113, 21477-21483.	1.5	50
79	Kinetic Isotope Effects in a Câ~'H Bond Dissociation by the Iron-Oxo Species of Cytochrome P450. Journal of Physical Chemistry B, 2000, 104, 12365-12370.	1.2	49
80	DFT Study on Chemical N ₂ Fixation by Using a Cubane-Type Rulr ₃ S ₄ Cluster: Energy Profile for Binding and Reduction of N ₂ to Ammonia via Ruâ^'Nâ^'NH _{<i>x</i>} (<i>x</i> = 1â^'3) Intermediates with Unique Structures. Journal of the American Chemical Society, 2008, 130, 9037-9047.	6.6	49
81	Photochemical Reversibility of Ring-Closing and Ring-Opening Reactions in Diarylperfluorocyclopentenes. Journal of Physical Chemistry C, 2009, 113, 3826-3834.	1.5	48
82	Molybdenum-Catalyzed Ammonia Formation Using Simple Monodentate and Bidentate Phosphines as Auxiliary Ligands. Inorganic Chemistry, 2019, 58, 8927-8932.	1.9	48
83	Methane Activation at the Metal–Support Interface of Ni ₄ –CeO ₂ (111) Catalyst: A Theoretical Study. Journal of Physical Chemistry C, 2019, 123, 9788-9798.	1.5	48
84	Mechanistic Insights into Homogeneous Electrocatalytic and Photocatalytic Hydrogen Evolution Catalyzed by High-Spin Ni(II) Complexes with S ₂ N ₂ -Type Tetradentate Ligands. Inorganic Chemistry, 2018, 57, 7180-7190.	1.9	47
85	Methane Hydroxylation on a Diiron Model of Soluble Methane Monooxygenase. Bulletin of the Chemical Society of Japan, 1998, 71, 1899-1909.	2.0	46
86	Directional Electron Transfer in Crystals of [CrCo] Dinuclear Complexes Achieved by Chirality-Assisted Preparative Method. Journal of the American Chemical Society, 2016, 138, 14170-14173.	6.6	46
87	An Azuleneâ€Fused Tetracene Diimide with a Small HOMO–LUMO Gap. ChemPlusChem, 2017, 82, 1010-1014.	1.3	45
88	Ground-State Copper(III) Stabilized by N-Confused/N-Linked Corroles: Synthesis, Characterization, and Redox Reactivity. Journal of the American Chemical Society, 2018, 140, 6883-6892.	6.6	45
89	Molecular understanding of the adhesive interactions between silica surface and epoxy resin: Effects of interfacial water. Journal of Computational Chemistry, 2019, 40, 164-171.	1.5	45
90	Adhesion of Epoxy Resin with Hexagonal Boron Nitride and Graphite. ACS Omega, 2019, 4, 4491-4504.	1.6	43

#	Article	IF	CITATIONS
91	Analysis of Photoinduced Magnetization in a (Co, Fe) Prussian Blue Model. Journal of Physical Chemistry B, 1998, 102, 5432-5437.	1.2	42
92	Macroscopic Polarization Change via Electron Transfer in a Valence Tautomeric Cobalt Complex. Nature Communications, 2020, 11, 1992.	5.8	41
93	Plasma polymerization of 1â€benzothiophene. Journal of Applied Physics, 1991, 70, 5653-5660.	1.1	40
94	Femtosecond Dynamics of the Methaneâ^'Methanol and Benzeneâ^'Phenol Conversions by an Ironâ^'Oxo Species. Journal of Physical Chemistry A, 2000, 104, 2552-2561.	1.1	40
95	Conductance through Short DNA Molecules. Journal of Physical Chemistry C, 2011, 115, 3481-3490.	1.5	40
96	Molecular design of electron transport with orbital rule: toward conductance-decay free molecular junctions. Physical Chemistry Chemical Physics, 2015, 17, 32099-32110.	1.3	40
97	Computational Exploration of the Mechanism of the Hydrogenation Step of the Anthraquinone Process for Hydrogen Peroxide Production. Journal of Physical Chemistry C, 2015, 119, 8748-8754.	1.5	40
98	Orbital Control of Single-Molecule Conductance Perturbed by π-Accepting Anchor Groups: Cyanide and Isocyanide. Journal of Physical Chemistry C, 2012, 116, 20607-20616.	1.5	39
99	Selective carbon dioxide adsorption of ε-Keggin-type zincomolybdate-based purely inorganic 3D frameworks. Journal of Materials Chemistry A, 2015, 3, 746-755.	5.2	39
100	A New Family of Anionic Fe ^{III} Spin Crossover Complexes Featuring a Weakâ€Field N ₂ O ₄ Coordination Octahedron. Chemistry - A European Journal, 2016, 22, 1253-1257.	1.7	39
101	Azaferroceneâ€Based PNPâ€Type Pincer Ligand: Synthesis of Molybdenum, Chromium, and Iron Complexes and Reactivity toward Nitrogen Fixation. European Journal of Inorganic Chemistry, 2016, 2016, 4856-4861.	1.0	39
102	Giant anisotropic thermal expansion actuated by thermodynamically assisted reorientation of imidazoliums in a single crystal. Nature Communications, 2019, 10, 4805.	5.8	39
103	Molecular Rectifier Based on ï€â€"ï€ Stacked Charge Transfer Complex. Journal of Physical Chemistry C, 2012, 116, 2575-2580.	1.5	38
104	Disilaruthena- and Ferracyclic Complexes Containing Isocyanide Ligands as Effective Catalysts for Hydrogenation of Unfunctionalized Sterically Hindered Alkenes. Journal of the American Chemical Society, 2018, 140, 4119-4134.	6.6	38
105	Mechanistic Proposals for Direct Benzene Hydroxylation over Feâ^'ZSM-5 Zeolite. Journal of Physical Chemistry B, 2003, 107, 11404-11410.	1.2	37
106	Formation and characterization of a reactive chromium(<scp>v</scp>)–oxo complex: mechanistic insight into hydrogen-atom transfer reactions. Chemical Science, 2015, 6, 945-955.	3.7	37
107	Dioxygen Activation on Cu-MOR Zeolite: Theoretical Insights into the Formation of Cu ₂ O and Cu ₃ O ₃ Active Species. Inorganic Chemistry, 2018, 57, 10146-10152.	1.9	37
108	Role of Hydrogen-Bonding and OHâ [~] ï€ Interactions in the Adhesion of Epoxy Resin on Hydrophilic Surfaces. ACS Omega, 2020, 5, 26211-26219.	1.6	36

#	Article	IF	CITATIONS
109	Quantum Transport Effects in Nanosized Graphite Sheets. II. Enhanced Transport Effects by Heteroatoms. Journal of Physical Chemistry B, 2003, 107, 8789-8793.	1.2	35
110	Mechanistic aspects in the direct synthesis of hydrogen peroxide on PdAu catalyst from first principles. Catalysis Today, 2015, 248, 142-148.	2.2	35
111	Molecular Orbital Interactions in the Nanostar Dendrimer. Journal of Physical Chemistry B, 2003, 107, 14204-14210.	1.2	34
112	QM/MM Study on the Catalytic Mechanism of Benzene Hydroxylation over Feâ^'ZSM-5. Organometallics, 2006, 25, 3118-3123.	1.1	34
113	Theoretical Study of Thermal Spin Transition between the Singlet State and the Quintet State in the [Fe(2-picolylamine)3]2+Spin Crossover System. Journal of Physical Chemistry A, 2010, 114, 5862-5869.	1.1	34
114	A Ruthenium(III)–Oxyl Complex Bearing Strong Radical Character. Angewandte Chemie - International Edition, 2016, 55, 14041-14045.	7.2	34
115	Heterometallic Fe ^{III} /K Coordination Polymer with a Wide Thermal Hysteretic Spin Transition at Room Temperature. Chemistry - A European Journal, 2016, 22, 532-538.	1.7	34
116	Mechanism for the Direct Oxidation of Benzene to Phenol by FeO+. Organometallics, 2005, 24, 3532-3538.	1.1	33
117	Role of Acidic Proton in the Decomposition of NO over Dimeric Cu(I) Active Sites in Cu-ZSM-5 Catalyst: A QM/MM Study. ACS Catalysis, 2014, 4, 2075-2085.	5.5	33
118	Hydrogen atom abstraction reactions independent of C–H bond dissociation energies of organic substrates in water: significance of oxidant–substrate adduct formation. Chemical Science, 2014, 5, 1429-1436.	3.7	33
119	Visible light-driven cross-coupling reactions of alkyl halides with phenylacetylene derivatives for C(sp ³)–C(sp) bond formation catalyzed by a B ₁₂ complex. Chemical Communications, 2019, 55, 13070-13073.	2.2	33
120	Catalytic C–H amination driven by intramolecular ligand-to-nitrene one-electron transfer through a rhodium(<scp>iii</scp>) centre. Chemical Communications, 2017, 53, 4849-4852.	2.2	32
121	Theoretical Investigation of Methane Hydroxylation over Isoelectronic [FeO] ²⁺ - and [MnO] ⁺ -Exchanged Zeolites Activated by N ₂ O. Inorganic Chemistry, 2017, 56, 10370-10380.	1.9	32
122	The Role of Orbital Interactions in Determining the Interlayer Spacing in Graphite Slabs. Journal of the American Chemical Society, 2000, 122, 11871-11875.	6.6	31
123	Mechanism for the Formaldehyde to Formic Acid and the Formic Acid to Carbon Dioxide Conversions Mediated by an Iron-Oxo Species. Journal of Physical Chemistry A, 2002, 106, 621-630.	1.1	31
124	Reverse Exponential Decay of Electrical Transmission in Nanosized Graphite Sheets. Journal of Physical Chemistry B, 2004, 108, 7565-7572.	1.2	31
125	Intraprotein transmethylation via a CH ₃ –Co(<scp>iii</scp>) species in myoglobin reconstituted with a cobalt corrinoid complex. Dalton Transactions, 2016, 45, 3277-3284.	1.6	31
126	Theoretical Measurements of Conductance in an (AT)12 DNA Molecule. ChemPhysChem, 2003, 4, 1256-1260.	1.0	30

#	Article	IF	CITATIONS
127	Anisotropic Change in the Magnetic Susceptibility of a Dynamic Single Crystal of a Cobalt(II) Complex. Angewandte Chemie - International Edition, 2017, 56, 717-721.	7.2	30
128	DFT exploration of active site motifs in methane hydroxylation by Ni-ZSM-5 zeolite. Catalysis Science and Technology, 2018, 8, 5875-5885.	2.1	30
129	Mechanistic Insight into Concerted Proton–Electron Transfer of a Ru(IV)-Oxo Complex: A Possible Oxidative Asynchronicity. Journal of the American Chemical Society, 2020, 142, 16982-16989.	6.6	30
130	DFT Study on N2 Activation by a Hydride-Bridged Diniobium Complex. N≡N Bond Cleavage Accompanied by H2 Evolution. Inorganic Chemistry, 2009, 48, 3875-3881.	1.9	29
131	Current Rectification through ï€â€"ï€ Stacking in Multilayered Donor–Acceptor Cyclophanes. Journal of Physical Chemistry C, 2012, 116, 26625-26635.	1.5	28
132	Possible Peroxo State of the Dicopper Site of Particulate Methane Monooxygenase from Combined Quantum Mechanics and Molecular Mechanics Calculations. Inorganic Chemistry, 2016, 55, 2771-2775.	1.9	28
133	Frontier Orbital Perspective for Quantum Interference in Alternant and Nonalternant Hydrocarbons. Journal of Physical Chemistry C, 2017, 121, 9621-9626.	1.5	28
134	Synthesis and reactivity of titanium- and zirconium-dinitrogen complexes bearing anionic pyrrole-based PNP-type pincer ligands. Dalton Transactions, 2018, 47, 11322-11326.	1.6	28
135	Quenching and Restoration of Orbital Angular Momentum through a Dynamic Bond in a Cobalt(II) Complex. Journal of the American Chemical Society, 2020, 142, 11434-11441.	6.6	28
136	Nickel-Catalyzed Reactions of Benzo[1,2:4,5]bis(1,1,2,2-tetraethyl-1,2-disilacyclobut-3-ene) with Alkynes and Ketones. Organometallics, 1999, 18, 4524-4529.	1.1	27
137	Siliconâ^'Carbon Unsaturated Compounds. 65. Thermal and Photochemical Isomerization of Trimethylsiloxy- and Bis(trimethylsilyl)-Substituted Silacyclobut-3-enesâ€. Organometallics, 2002, 21, 2033-2035.	1.1	27
138	Density-Functional Tight-Binding Study on the Effects of Interfacial Water in the Adhesion Force between Epoxy Resin and Alumina Surface. Langmuir, 2018, 34, 14428-14438.	1.6	27
139	Optimization of Work Function via Bayesian Machine Learning Combined with First-Principles Calculation. Journal of Physical Chemistry C, 2020, 124, 9958-9970.	1.5	27
140	Role of molecular distortions in the spin–orbit coupling between the singlet and triplet states of the 4ï€ electron systems C4H4, C5H5+, and C3H3â^. Journal of Chemical Physics, 2001, 115, 9243-9254.	1.2	26
141	Catalytic reduction of dinitrogen to tris(trimethylsilyl)amine using rhodium complexes with a pyrrole-based PNP-type pincer ligand. Chemical Communications, 2019, 55, 14886-14889.	2.2	26
142	Orbital view concept applied on photoswitching systems. Thin Solid Films, 2009, 518, 444-447.	0.8	25
143	Thermally Induced Intraâ€Carboxyl Proton Shuttle in a Molecular Rackâ€andâ€Pinion Cascade Achieving Macroscopic Crystal Deformation. Angewandte Chemie - International Edition, 2016, 55, 14628-14632.	7.2	25
144	A Squareâ€Planar Complex of Platinum(0). Angewandte Chemie - International Edition, 2016, 55, 15347-15350.	7.2	25

#	Article	IF	CITATIONS
145	Prediction of the Glass-Transition Temperatures of Linear Homo/Heteropolymers and Cross-Linked Epoxy Resins. ACS Applied Polymer Materials, 2019, 1, 1430-1442.	2.0	25
146	Cycling between Molybdenumâ€Ðinitrogen and â€Nitride Complexes to Support the Reaction Pathway for Catalytic Formation of Ammonia from Dinitrogen. Chemistry - A European Journal, 2020, 26, 13383-13389.	1.7	25
147	Title is missing!. Molecular Engineering, 1999, 8, 357-373.	0.2	24
148	Interaction of SrO-terminated SrTiO ₃ surface with oxygen, carbon dioxide, and water. Journal of Materials Chemistry A, 2018, 6, 22662-22672.	5.2	24
149	Catalytic Reactivity of Molybdenum–Trihalide Complexes Bearing PCPâ€Type Pincer Ligands. Chemistry - an Asian Journal, 2019, 14, 2091-2096.	1.7	24
150	Novel Mechanistic Insights into Methane Activation over Fe and Cu Active Sites in Zeolites: A Comparative DFT Study Using Meta-GGA Functionals. Journal of Physical Chemistry C, 2020, 124, 18112-18125.	1.5	24
151	Electron Correlation Effects and PossibleD6hStructures in Large Cyclic Polyenes. The Journal of Physical Chemistry, 1996, 100, 5697-5701.	2.9	23
152	Synthesis and Platinum- and Palladium-Catalyzed Reactions of Benzo[1,2:4,5]bis(1,1,2,2-tetraethyl-1,2-disilacyclobut-3-ene). Organometallics, 1998, 17, 5830-5835.	1.1	23
153	Orbital Views on Electron-Transport Properties of Cyclophanes: Insight into Intermolecular Transport. Bulletin of the Chemical Society of Japan, 2012, 85, 181-188.	2.0	23
154	Energetic Mechanism of Cytochrome c-Cytochrome c Oxidase Electron Transfer Complex Formation under Turnover Conditions Revealed by Mutational Effects and Docking Simulation. Journal of Biological Chemistry, 2016, 291, 15320-15331.	1.6	23
155	Low-Mode Conformational Search Method with Semiempirical Quantum Mechanical Calculations: Application to Enantioselective Organocatalysis. Journal of Chemical Information and Modeling, 2016, 56, 347-353.	2.5	23
156	Observation of Proton Transfer Coupled Spin Transition and Trapping of Photoinduced Metastable Proton Transfer State in an Fe(II) Complex. Journal of the American Chemical Society, 2019, 141, 14384-14393.	6.6	23
157	Ab Initio Study on Interaction and Stability of Lithiumâ€Đoped Amorphous Carbons. Journal of the Electrochemical Society, 1999, 146, 1262-1269.	1.3	22
158	Current Rectification in Nitrogen- and Boron-Doped Nanographenes and Cyclophanes. Journal of Physical Chemistry C, 2012, 116, 18451-18459.	1.5	22
159	Mechanistic Insights into C–H Oxidations by Ruthenium(III)-Pterin Complexes: Impact of Basicity of the Pterin Ligand and Electron Acceptability of the Metal Center on the Transition States. Journal of the American Chemical Society, 2016, 138, 9508-9520.	6.6	22
160	Redox Potentials of Cobalt Corrinoids with Axial Ligands Correlate with Heterolytic Co–C Bond Dissociation Energies. Inorganic Chemistry, 2017, 56, 1950-1955.	1.9	22
161	Synergy of Electrostatic and van der Waals Interactions in the Adhesion of Epoxy Resin with Carbon-Fiber and Class Surfaces. Bulletin of the Chemical Society of Japan, 2017, 90, 500-505.	2.0	22
162	Synthesis and Stereochemistry of cis- and trans-3,4- Benzo-1,2-di(tert-butyl)-1,2-dimethyl-1,2-disilacyclobutene. Organometallics, 2001, 20, 1059-1061.	1.1	21

#	Article	IF	CITATIONS
163	Quantum Chemical Studies on Dioxygen Activation and Methane Hydroxylation by Diiron and Dicopper Species as well as Related Metal–Oxo Species. Bulletin of the Chemical Society of Japan, 2013, 86, 1083-1116.	2.0	21
164	Formation and High Reactivity of the <i>anti</i> â€Dioxo Form of Highâ€Spin μâ€Oxodioxodiiron(IV) as the Active Species That Cleaves Strong Câ^'H Bonds. Chemistry - A European Journal, 2016, 22, 5924-5936.	1.7	21
165	Photochemical Intramolecular Câ^'H Addition of Dimesityl(hetero)arylboranes through a [1,6]â€5igmatropic Rearrangement. Angewandte Chemie - International Edition, 2017, 56, 12210-12214.	7.2	21
166	Esterification of Tertiary Amides by Alcohols Through Câ^'N Bond Cleavage over CeO ₂ . ChemCatChem, 2019, 11, 449-456.	1.8	21
167	An Azulene-Based Chiral Helicene and Its Air-Stable Cation Radical. Bulletin of the Chemical Society of Japan, 2019, 92, 1867-1873.	2.0	21
168	Room-Temperature Activation of Methane and Direct Formations of Acetic Acid and Methanol on Zn-ZSM-5 Zeolite: A Mechanistic DFT Study. Bulletin of the Chemical Society of Japan, 2020, 93, 345-354.	2.0	21
169	Ammonia Formation Catalyzed by a Dinitrogenâ€Bridged Dirhenium Complex Bearing PNPâ€Pincer Ligands under Mild Reaction Conditions**. Angewandte Chemie - International Edition, 2021, 60, 13906-13912.	7.2	21
170	Manipulating electron redistribution to achieve electronic pyroelectricity in molecular [FeCo] crystals. Nature Communications, 2021, 12, 4836.	5.8	21
171	Regioselectivity in 2-Methylbutane Hydroxylation Mediated by FeO+ and FeO2+. Organometallics, 2001, 20, 1397-1407.	1.1	20
172	Catalytic Reduction of Molecular Dinitrogen to Ammonia and Hydrazine Using Vanadium Complexes. Angewandte Chemie, 2018, 130, 9202-9206.	1.6	20
173	Catalytic Performance of a Dicopper–Oxo Complex for Methane Hydroxylation. Inorganic Chemistry, 2018, 57, 8-11.	1.9	20
174	Thermochemistry and Kinetics of the Thermal Degradation of 2-Methoxyethanol as Possible Biofuel Additives. Scientific Reports, 2019, 9, 4535.	1.6	20
175	Synthesis, spectral characterization, density functional theory studies, and biological screening of some transition metal complexes of a novel hydrazide–hydrazone ligand of isonicotinic acid. Applied Organometallic Chemistry, 2021, 35, e6205.	1.7	20
176	One-Pot Synthesis of Tertiary Amides from Organic Trichlorides through Oxygen Atom Incorporation from Air by Convergent Paired Electrolysis. Journal of Organic Chemistry, 2021, 86, 5983-5990.	1.7	20
177	Orbital views of the electron transport through heterocyclic aromatic hydrocarbons. Theoretical Chemistry Accounts, 2011, 130, 765-774.	0.5	19
178	Roles of carboxylate donors in O–O bond scission of peroxodi-iron(<scp>iii</scp>) to high-spin oxodi-iron(<scp>iv</scp>) with a new carboxylate-containing dinucleating ligand. Chemical Science, 2014, 5, 2282-2292.	3.7	19
179	Proton-Assisted Mechanism of NO Reduction on a Dinuclear Ruthenium Complex. Inorganic Chemistry, 2015, 54, 7181-7191.	1.9	19
180	Cupric-superoxide complex that induces a catalytic aldol reaction-type C–C bond formation. Communications Chemistry, 2019, 2, .	2.0	19

#	Article	IF	CITATIONS
181	Theoretical Study on the Contribution of Interfacial Functional Groups to the Adhesive Interaction between Epoxy Resins and Aluminum Surfaces. Langmuir, 2022, 38, 6653-6664.	1.6	19
182	First-Principles Calculations of Electron Transport through Azulene. Journal of Physical Chemistry C, 2016, 120, 9043-9052.	1.5	18
183	Theoretical Study of the Catalytic Hydrogenation of Alkenes by a Disilaferracyclic Complex: Can the Fe–Si σ-Bond-Assisted Activation of H–H Bonds Allow Development of a Catalysis of Iron?. Journal of Organic Chemistry, 2016, 81, 10900-10911.	1.7	18
184	Theoretical Study on the Adhesion Interaction between Epoxy Resin Including Curing Agent and Plated Gold Surface. Langmuir, 2021, 37, 3982-3995.	1.6	18
185	Cobalt–Carbon Bond Formation Reaction via Ligand Reduction of Porphycene–Cobalt(II) Complex and Its Noninnocent Reactivity. ACS Omega, 2018, 3, 4027-4034.	1.6	17
186	Contribution of Coulomb Interactions to a Two-Step Crystal Structure Phase Transformation Coupled with a Significant Change in Spin Crossover Behavior for a Series of Charged Fe ^{II} Complexes from 2,6-Bis(2-methylthiazol-4-yl)pyridine. Inorganic Chemistry, 2018, 57, 1277-1287.	1.9	17
187	Computational Studies on the Thermodynamic and Kinetic Parameters of Oxidation of 2-Methoxyethanol Biofuel via H-Atom Abstraction by Methyl Radical. Scientific Reports, 2019, 9, 15361.	1.6	17
188	Nitrogen Fixation Catalyzed by Dinitrogenâ€Bridged Dimolybdenum Complexes Bearing PCP―and PNPâ€Type Pincer Ligands: A Shortcut Pathway Deduced from Free Energy Profiles. European Journal of Inorganic Chemistry, 2020, 2020, 1490-1498.	1.0	17
189	Theoretical Study of the Direct Conversion of Methane to Methanol Using H ₂ O ₂ as an Oxidant on Pd and Au/Pd Surfaces. Journal of Physical Chemistry C, 2020, 124, 13231-13239.	1.5	17
190	Competition between Hydrogen Bonding and Dispersion Force in Water Adsorption and Epoxy Adhesion to Boron Nitride: From the Flat to the Curved. Langmuir, 2021, 37, 11351-11364.	1.6	17
191	Preparation and reactivity of molybdenum complexes bearing pyrrole-based PNP-type pincer ligand. Chemical Communications, 2020, 56, 6933-6936.	2.2	17
192	A stability condition for the Hartree–Fock solution of the infinite oneâ€dimensional system. Journal of Chemical Physics, 1989, 91, 3724-3728.	1.2	16
193	Quantum-size effects in capped and uncapped carbon nanotubes. Annual Reports on the Progress of Chemistry Section C, 2006, 102, 71.	4.4	16
194	Orbital Determining Spintronic Properties of a π-Conjugated System. Journal of Physical Chemistry C, 2012, 116, 16325-16332.	1.5	16
195	Redox-Noninnocent Behavior of Tris(2-pyridylmethyl)amine Bound to a Lewis Acidic Rh(III) Ion Induced by C–H Deprotonation. Journal of the American Chemical Society, 2015, 137, 11222-11225.	6.6	16
196	Crystal Structures and Coordination Behavior of Aqua- and Cyano-Co(III) Tetradehydrocorrins in the Heme Pocket of Myoglobin. Inorganic Chemistry, 2016, 55, 1287-1295.	1.9	16
197	Persistent four-coordinate iron-centered radical stabilized by π-donation. Chemical Science, 2016, 7, 191-198.	3.7	16
198	Lithium-Richest Phase of Lithium Tetrelides Li17Tt4 (Tt = Si, Ge, Sn, and Pb) as an Electride. Bulletin of the Chemical Society of Japan, 2019, 92, 1154-1169.	2.0	16

#	Article	IF	CITATIONS
199	The Role of Coulomb Interactions for Spin Crossover Behaviors and Crystal Structural Transformation in Novel Anionic Fe(III) Complexes from a π-Extended ONO Ligand. Crystals, 2016, 6, 49.	1.0	15
200	Three‣tep Spin State Transition and Hysteretic Proton Transfer in the Crystal of an Iron(II) Hydrazone Complex. Angewandte Chemie - International Edition, 2020, 59, 14781-14787.	7.2	15
201	Energy Decomposition Analysis of the Adhesive Interaction between an Epoxy Resin Layer and a Silica Surface. Langmuir, 2021, 37, 8417-8425.	1.6	15
202	A Theoretical Study of Dioxygen Activation on the Dicopper Enzyme Model. Bulletin of the Chemical Society of Japan, 1997, 70, 1911-1917.	2.0	14
203	QM/MM Study of the Mononuclear Non-Heme Iron Active Site of Phenylalanine Hydroxylase. Journal of Physical Chemistry B, 2004, 108, 17226-17237.	1.2	14
204	Molecular Theory of Adhesion of Metal/Epoxy Resin Interface. Kobunshi Ronbunshu, 2011, 68, 72-80.	0.2	14
205	Real-space observation of far- and near-field-induced photolysis of molecular oxygen on an Ag(110) surface by visible light. Journal of Chemical Physics, 2019, 151, 144705.	1.2	14
206	Vibronic Interactions in Silicon Polyhedra of the Si46Clathrate Compound. Journal of Physical Chemistry A, 1998, 102, 10113-10119.	1.1	13
207	Theoretical Study on Activation and Protonation of Dinitrogen on Cubane-Type MIr ₃ S ₄ Clusters (M = V, Cr, Mn, Fe, Co, Ni, Cu, Mo, Ru, and W). Inorganic Chemistry, 2010, 49, 2464-2470.	1.9	13
208	<i>cis</i> -1,2-Aminohydroxylation of Alkenes Involving a Catalytic Cycle of Osmium(III) and Osmium(V) Centers: Os ^V (O)(NHTs) Active Oxidant with a Macrocyclic Tetradentate Ligand. Inorganic Chemistry, 2015, 54, 7073-7082.	1.9	13
209	Electrical Conductance and Diode-Like Behavior of Substituted Azulene. Journal of Physical Chemistry C, 2017, 121, 2504-2511.	1.5	13
210	Thermodynamics and Photodynamics of a Monoprotonated Porphyrin Directly Stabilized by Hydrogen Bonding with Polar Protic Solvents. Chemistry - A European Journal, 2017, 23, 4669-4679.	1.7	13
211	Acid–Base Properties of a Freebase Form of a Quadruply Ring-Fused Porphyrin—Stepwise Protonation Induced by Rigid Ring-Fused Structure. Journal of Organic Chemistry, 2017, 82, 322-330.	1.7	13
212	Intermediate-Spin Iron(III) Complexes Having a Redox-Noninnocent Macrocyclic Tetraamido Ligand. Inorganic Chemistry, 2018, 57, 9683-9695.	1.9	13
213	Combined theoretical and experimental study on alcoholysis of amides on CeO2 surface: A catalytic interplay between Lewis acid and base sites. Catalysis Today, 2018, 303, 256-262.	2.2	13
214	Synthesis and Catalytic Reactivity of Bis(molybdenum-trihalide) Complexes Bridged by Ferrocene Skeleton toward Catalytic Nitrogen Fixation. Organometallics, 2019, 38, 2863-2872.	1.1	13
215	Mixed-Anion Control of C–H Bond Activation of Methane on the IrO2 Surface. Journal of Physical Chemistry C, 2020, 124, 17058-17072.	1.5	13
216	Electronic Origin of Catalytic Activity of TiH ₂ for Ammonia Synthesis. Journal of Physical Chemistry C, 2021, 125, 3948-3960.	1.5	13

#	Article	IF	CITATIONS
217	Elucidation of Adhesive Interaction between the Epoxy Molding Compound and Cu Lead Frames. ACS Omega, 2021, 6, 34173-34184.	1.6	13
218	Catalytic Reduction of Dinitrogen into Ammonia and Hydrazine by Using Chromium Complexes Bearing PCPâ€Type Pincer Ligands**. Chemistry - A European Journal, 2022, 28, .	1.7	13
219	Molecular Orbital Study on Quartet Molecules with Trigonal Axis of Symmetry. Molecular Crystals and Liquid Crystals, 1993, 232, 323-332.	0.3	12
220	Possible Nitrogen Fixation by Disilabutadiene. Organometallics, 1997, 16, 5058-5063.	1.1	12
221	Vibronic Interaction in Metalloporphyrin π-Anion Radicals. Journal of Physical Chemistry A, 2007, 111, 852-857.	1.1	12
222	Fundamental electron-transfer and proton-coupled electron-transfer properties of Ru(iv)-oxo complexes. Dalton Transactions, 2019, 48, 13154-13161.	1.6	12
223	Temperature dependence of spherical electron transfer in a nanosized [Fe14] complex. Nature Communications, 2019, 10, 5510.	5.8	12
224	Bonding of C ₁ fragments on metal nanoclusters: a search for methane conversion catalysts with swarm intelligence. Physical Chemistry Chemical Physics, 2021, 23, 14004-14015.	1.3	12
225	High-Temperature Cooperative Spin Crossover Transitions and Single-Crystal Reflection Spectra of [FeIII(qsal)2](CH3OSO3) and Related Compounds. Crystals, 2019, 9, 81.	1.0	11
226	Photocatalytic hydrogen evolution using a Ru(ii)-bound heteroaromatic ligand as a reactive site. Dalton Transactions, 2020, 49, 17230-17242.	1.6	11
227	Local Structures and Dynamics of Imidazole Molecules in Poly(vinylphosphonic acid)–Imidazole Composite Investigated by Molecular Dynamics. ACS Applied Polymer Materials, 2020, 2, 1561-1568.	2.0	11
228	Understanding Single-Molecule Parallel Circuits on the Basis of Frontier Orbital Theory. Journal of Physical Chemistry C, 2020, 124, 3322-3331.	1.5	11
229	Catalytic Reduction of Dinitrogen to Ammonia and Hydrazine Using Iron–Dinitrogen Complexes Bearing Anionic Benzene-Based PCP-Type Pincer Ligands. Bulletin of the Chemical Society of Japan, 2022, 95, 683-692.	2.0	11
230	Mechanistic Study for the Reaction of B ₁₂ Complexes with <i>m</i> -Chloroperbenzoic Acid in Catalytic Alkane Oxidations. Inorganic Chemistry, 2022, 61, 9710-9724.	1.9	11
231	Orbital Interactions and Solvent Effects Determining the Stability of Condensed Cyclopentadienides in Solution. Journal of Organic Chemistry, 1999, 64, 2821-2829.	1.7	10
232	The chemistry of benzodisilacyclobutenes and benzobis(disilacyclobutene)s: new development of transition-metal-catalyzed reactions, stereochemistry and theoretical studies. Dalton Transactions, 2016, 45, 3210-3235.	1.6	10
233	Formation and Isolation of a Fourâ€Electronâ€Reduced Porphyrin Derivative by Reduction of a Stable 20Ï€ Isophlorin. Angewandte Chemie - International Edition, 2018, 57, 1973-1977.	7.2	10
234	Theoretical Study on the Electronic Structure of Heavy Alkali-Metal Suboxides. Inorganic Chemistry, 2020, 59, 1340-1354.	1.9	10

#	Article	IF	CITATIONS
235	Electronic and Optical Modulation of Metal-Doped Hybrid Organic–Inorganic Perovskites Crystals by Post-Treatment Control. ACS Applied Energy Materials, 2020, 3, 7500-7511.	2.5	10
236	Comparative study of the ideal and actual adhesion interfaces of the die bonding structure using conductive adhesives. Journal of Adhesion, 2020, , 1-25.	1.8	10
237	Anthranoxides as Highly Reactive Arynophiles for the Synthesis of Triptycenes. Chemistry - A European Journal, 2020, 26, 8506-8510.	1.7	10
238	Computational Study on Stable Structures, Formation Energies, and Conductance of Single Benzene-dithiolate between Two Au Electrodes. Japanese Journal of Applied Physics, 2005, 44, 7729-7731.	0.8	9
239	Siliconâ~Carbon Unsaturated Compounds. 76. Photochemical and Thermal Behavior of 1-Silacyclobut-3-enes Generated from the Reaction of Pivaloyltris(trimethylsilyl)silane with <i>tert</i> -Butylacetylene. Organometallics, 2009, 28, 5641-5646.	1.1	9
240	Mixed-metal complex [Fe(bipe)(Au(CN)2)2·MeOH] with gold clusters: a novel two-dimensional polyrotaxane net clipped by aurophilic interaction. CrystEngComm, 2010, 12, 4031.	1.3	9
241	<i>`İf </i> -CAM Mechanisms for the Hydrogenation of Alkenes by <i>cis</i> - and <i>trans</i> -Disilametallacyclic Carbonyl Complexes (M = Fe, Ru, Os): Experimental and Theoretical Studies. Bulletin of the Chemical Society of Japan, 2017, 90, 613-626.	2.0	9
242	Aerobic oxidation of alkanes on icosahedron gold nanoparticle Au55. Journal of Catalysis, 2018, 364, 141-153.	3.1	9
243	Mechanical Control of Molecular Conductance and Diradical Character in Bond Stretching and ï€-Stack Compression. Journal of Physical Chemistry C, 2020, 124, 22941-22958.	1.5	9
244	Iridium-catalyzed Formation of Silylamine from Dinitrogen under Ambient Reaction Conditions. Chemistry Letters, 2020, 49, 794-797.	0.7	9
245	Structural characterization of molybdenum–dinitrogen complex as key species toward ammonia formation by dispersive XAFS spectroscopy. Physical Chemistry Chemical Physics, 2020, 22, 12368-12372.	1.3	9
246	Mixed Anion Control of the Partial Oxidation of Methane to Methanol on the β-PtO ₂ Surface. ACS Omega, 2021, 6, 13858-13869.	1.6	9
247	Push–pull fluorenones and benzazulenequinones: regioselective [4+2] and [2+2] cycloadditions of benzopentalenequinone derivative and alkynes bearing an aniline moiety. Tetrahedron Letters, 2016, 57, 4604-4607.	0.7	8
248	Trithiazolyl-1,3,5-triazines bearing decyloxybenzene moieties: synthesis, photophysical and electrochemical properties, and self-assembly behavior. Organic and Biomolecular Chemistry, 2018, 16, 3584-3595.	1.5	8
249	Importance of the Reactant-State Potentials of Chromium(V)–Oxo Complexes to Determine the Reactivity in Hydrogen-Atom Transfer Reactions. Inorganic Chemistry, 2018, 57, 13929-13936.	1.9	8
250	Role of Amino Acid Residues for Dioxygen Activation in the Second Coordination Sphere of the Dicopper Site of pMMO. Inorganic Chemistry, 2019, 58, 12280-12288.	1.9	8
251	Formation of a Ruthenium(V)—Imido Complex and the Reactivity in Substrate Oxidation in Water through the Nitrogen Non-Rebound Mechanism. Inorganic Chemistry, 2019, 58, 12815-12824.	1.9	8
252	Mechanistic Study on Catalytic Disproportionation of Hydrazine by a Protic Pincerâ€Type Iron Complex through Protonâ€Coupled Electron Transfer. European Journal of Inorganic Chemistry, 2020, 2020, 1472-1482.	1.0	8

#	Article	IF	CITATIONS
253	Selective catalytic 2e ^{â^'} -oxidation of organic substrates by an Fe ^{II} complex having an N-heterocyclic carbene ligand in water. Chemical Communications, 2020, 56, 9783-9786.	2.2	8
254	Electrochemical Synthesis of Cyanoformamides from Trichloroacetonitrile and Secondary Amines Mediated by the B12 Derivative. Journal of Organic Chemistry, 2021, 86, 16134-16143.	1.7	8
255	S,C,C- and O,C,C-Bridged Triarylamines and Their Persistent Radical Cations. Journal of Organic Chemistry, 2021, 86, 12559-12568.	1.7	8
256	Synthesis and Reactivity of Cobalt–Dinitrogen Complexes Bearing Anionic PCP-Type Pincer Ligands toward Catalytic Silylamine Formation from Dinitrogen. Inorganic Chemistry, 2022, 61, 5190-5195.	1.9	8
257	Peel Adhesion Strength between Epoxy Resin and Hydrated Silica Surfaces: A Density Functional Theory Study. ACS Omega, 2022, 7, 17393-17400.	1.6	8
258	FERROMAGNETIC TDAE-C60 VERSUS PARAMAGNETIC TDAE-C70: FARADEY BALANCE AND ESR STUDY. International Journal of Modern Physics B, 1992, 06, 3953-3958.	1.0	7
259	Orbital Interaction Analysis of McConnell's Model for Through-Space Magnetic Coupling. Molecular Crystals and Liquid Crystals, 1997, 305, 157-166.	0.3	7
260	Theoretical Analysis of the Reaction Mechanism of Biotin Carboxylase. Journal of Chemical Theory and Computation, 2008, 4, 366-374.	2.3	7
261	A Bipodal Dicyano Anchor Unit for Singleâ€Molecule Spintronic Devices. ChemPhysChem, 2013, 14, 2470-2475.	1.0	7
262	Binding of Scandium Ions to Metalloporphyrin–Flavin Complexes for Long‣ived Charge Separation. Chemistry - A European Journal, 2014, 20, 15518-15532.	1.7	7
263	Computational Mutation Design of Diol Dehydratase: Catalytic Ability toward Glycerol beyond the Wild-Type Enzyme. Bulletin of the Chemical Society of Japan, 2014, 87, 950-959.	2.0	7
264	A Squareâ€Planar Complex of Platinum(0). Angewandte Chemie, 2016, 128, 15573-15576.	1.6	7
265	Photochemical Intramolecular Câ^H Addition of Dimesityl(hetero)arylboranes through a [1,6]â€5igmatropic Rearrangement. Angewandte Chemie, 2017, 129, 12378-12382.	1.6	7
266	Oxygen Atom Insertion into the Osmium–Carbon Bond via an Organometallic Oxido–Osmium(V) Intermediate. Organometallics, 2021, 40, 102-106.	1.1	7
267	Quadruple Role of Pd Catalyst in Domino Reaction Involving Aryl to Alkyl 1,5â€Pd Migration to Access 1,9â€Bridged Triptycenes. Chemistry - A European Journal, 2021, 27, 11548-11553.	1.7	7
268	Cubically cage-shaped mesoporous ordered silica for simultaneous visual detection and removal of uranium ions from contaminated seawater. Mikrochimica Acta, 2022, 189, 3.	2.5	7
269	Molecular Dynamics Study on the Thermal Aspects of the Effect of Water Molecules at the Adhesive Interface on an Adhesive Structure. Langmuir, 2021, 37, 14724-14732.	1.6	7
270	Effects of electron-phonon coupling on quantum interference in polyenes. Journal of Chemical Physics, 2018, 149, 134115.	1.2	6

#	Article	IF	CITATIONS
271	From Infection Clusters to Metal Clusters: Significance of the Lowest Occupied Molecular Orbital (LOMO). ACS Omega, 2021, 6, 1339-1351.	1.6	6
272	Distinct Behaviors of Cu- and Ni-ZSM-5 Zeolites toward the Post-activation Reactions of Methane. Journal of Physical Chemistry C, 2021, 125, 19333-19344.	1.5	6
273	Tin(II)–Nitrene Radical Complexes Formed by Electron Transfer from Redox-Active Ligand to Organic Azides and Their Reactivity in C(sp ³)–H Activation. Inorganic Chemistry, 2021, 60, 18603-18607.	1.9	6
274	DFT Study on the pH Dependence of the Reactivity of Ferrate(VI). ACS Symposium Series, 2016, , 473-487.	0.5	5
275	Catalyst Informatics on Methane Activation on Various Metal Alloys. Journal of Computer Chemistry Japan, 2017, 16, 147-148.	0.0	5
276	Two Discrete RuCp* (Cp*=Pentamethylcyclopentadienyl) Binding Modes of Nâ€Confused Porphyrins: Peripheral π Complex and Sitting Atop Ruthenocenophane Complex by Skeletal Transformation. Chemistry - A European Journal, 2018, 24, 6742-6746.	1.7	5
277	Effect of chemically induced permittivity changes on the plasmonic properties of metal nanoparticles. Communications Materials, 2021, 2, .	2.9	5
278	Halide-Adducts of OsO4. Structure and Reactivity in Alcohol-Oxidation. Bulletin of the Chemical Society of Japan, 2022, 95, 64-72.	2.0	5
279	Hydroboration and Hydrosilylation of a Molybdenum–Nitride Complex Bearing a PNP-Type Pincer Ligand. Organometallics, 2022, 41, 366-373.	1.1	5
280	Midgap levels of photoexcited conductive polymers. I. A simple description of the midgap levels based on molecular orbital interaction. International Journal of Quantum Chemistry, 1991, 40, 305-314.	1.0	4
281	First observation of clusters for solvated tropylium ions. Chemical Communications, 2001, , 1768-1769.	2.2	4
282	Asymmetric Diarylethene as a Dual-Functional Device Combining Switch and Diode. Bulletin of the Chemical Society of Japan, 2013, 86, 947-954.	2.0	4
283	A Study of Adhesion Interface about Die Bonding Structure with Conductive Silver Paste. , 2018, , .		4
284	Dual Catalytic Cycle of H2 and H2O Oxidations by a Half-Sandwich Iridium Complex: A Theoretical Study. Inorganic Chemistry, 2019, 58, 7274-7284.	1.9	4
285	Redox behaviour of the \hat{l}^2 -dihydroporphycene cobalt complex: study on the effect of hydrogenation of the ligand. Dalton Transactions, 2019, 48, 872-881.	1.6	4
286	Computational Study on the Light-Induced Oxidation of Iridium–Aqua Complex to Iridium–Oxo Complex over WO ₃ (001) Surface. Inorganic Chemistry, 2020, 59, 415-422.	1.9	4
287	Cycling between Molybdenumâ€Ðinitrogen and â€Nitride Complexes to Support the Reaction Pathway for Catalytic Formation of Ammonia from Dinitrogen. Chemistry - A European Journal, 2020, 26, 13321-13321.	1.7	4
288	Three‣tep Spin State Transition and Hysteretic Proton Transfer in the Crystal of an Iron(II) Hydrazone Complex. Angewandte Chemie, 2020, 132, 14891-14897.	1.6	4

#	Article	IF	CITATIONS
289	Chemical transformations of push–pull fluorenones: push–pull dibenzodicyanofulvenes as well as fluorenone– and dibenzodicyanofulvene–tetracyanobutadiene conjugates. Organic and Biomolecular Chemistry, 2020, 18, 4198-4209.	1.5	4
290	Active Catalyst for Methane Hydroxylation by an Iridium–Oxo Complex. ACS Catalysis, 2020, 10, 8254-8262.	5.5	4
291	Mechanistic Insights into the Dicopper-Complex-Catalyzed Hydroxylation of Methane and Benzene Using Nitric Oxide: A DFT Study. Inorganic Chemistry, 2021, 60, 4599-4609.	1.9	4
292	C(sp ³)–H bond activation by the carboxylate-adduct of osmium tetroxide (OsO ₄). Dalton Transactions, 2022, 51, 1123-1130.	1.6	4
293	Possible Photoinduced Spin Transitions in Bis(phenylmethylenyl)[2.2]paracyclophanes. A Spinâ^'Orbit Coupling Study. Journal of Physical Chemistry A, 2002, 106, 7915-7920.	1.1	3
294	Molecular functionalization of all-inorganic perovskite CsPbBr ₃ thin films. Journal of Materials Chemistry C, 2020, 8, 12587-12598.	2.7	3
295	Theoretical rationalization for the equilibrium between (μ–η ² :η ² -peroxido)Cu ^{II} Cu ^{II} and bis(μ-oxido)Cu ^{III} Cu ^{III} complexes: perturbational effects from ligand frameworks. Dalton Transactions. 2020. 49. 6710-6717.	1.6	3
296	Arylene–hexaynylene and –octaynylene macrocycles: extending the polyyne chains drives self-association by enhanced dispersion force. Chemical Communications, 2021, 57, 576-579.	2.2	3
297	Osmotic pressure effects identify dehydration upon cytochrome c–cytochrome c oxidase complex formation contributing to a specific electron pathway formation. Biochemical Journal, 2020, 477, 1565-1578.	1.7	3
298	Topology Dictates Magnetic and Conductive Properties of a ï€-Stacked System: Insight into Possible Coexistence of Magnetic and Conductive Systems. Journal of Physical Chemistry C, 2022, 126, 3244-3256.	1.5	3
299	Light-driven oxidation of CH ₄ to C ₁ chemicals catalysed by an organometallic Ru complex with O ₂ . RSC Advances, 2022, 12, 12253-12257.	1.7	3
300	Unrestricted Hartree-Fock method for infinite systems with antiferromagnetic array: Analysis of antiferromagnetic state oftrans-polyacetylene. International Journal of Quantum Chemistry, 1993, 45, 391-400.	1.0	2
301	Thermally Induced Intraâ€Carboxyl Proton Shuttle in a Molecular Rackâ€andâ€Pinion Cascade Achieving Macroscopic Crystal Deformation. Angewandte Chemie, 2016, 128, 14848-14852.	1.6	2
302	NH Tautomerism of a Quadruply Fused Porphyrin: Rigid Fused Structure Delays the Proton Transfer. Journal of Physical Chemistry B, 2018, 122, 316-327.	1.2	2
303	Electronic transport investigation of redox-switching of azulenequinones/hydroquinones <i>via</i> first-principles studies. Physical Chemistry Chemical Physics, 2019, 21, 17859-17867.	1.3	2
304	Mechanistic Study on Ringâ€Contracting Skeletal Rearrangement from Porphycene to Isocorrole by Experimental and Theoretical Methods. European Journal of Organic Chemistry, 2020, 2020, 1811-1816.	1.2	2
305	Attenuation of Redox Switching and Rectification in Azulenequinones/Hydroquinones after B and N Doping: A Firstâ€Principles Investigation. Advanced Theory and Simulations, 2021, 4, 2000203.	1.3	2
306	Ammonia Formation Catalyzed by a Dinitrogenâ€Bridged Dirhenium Complex Bearing PNPâ€Pincer Ligands under Mild Reaction Conditions**. Angewandte Chemie, 2021, 133, 14025-14031.	1.6	2

#	Article	IF	CITATIONS
307	Exploring Metal Cluster Catalysts Using Swarm Intelligence: Start with Hydrogen Adsorption. Topics in Catalysis, 2022, 65, 215-227.	1.3	2
308	Methane Hydroxylation by First Row Transition Metal Oxides. , 0, , 317-335.		2
309	Dynamics and Energetics of Methane on the Surfaces of Transition Metal Oxides. , 2020, , 101-133.		2
310	Graph-theoretical exploration of the relation between conductivity and connectivity in heteroatom-containing single-molecule junctions. Journal of Chemical Physics, 2022, 156, 091102.	1.2	2
311	Theoretical Investigation into Selective Benzene Hydroxylation by Ruthenium-Substituted Keggin-Type Polyoxometalates. Inorganic Chemistry, 2022, 61, 10-14.	1.9	2
312	Midgap levels of photoexcited conductive polymers. II. Detailed analysis oftrans-polyacetylene. International Journal of Quantum Chemistry, 1991, 40, 315-322.	1.0	1
313	A cluster model study of the electron–phonon interaction in magnesium diborate. Journal of Chemical Physics, 2001, 115, 7344-7347.	1.2	1
314	Thermal behavior of benzobis(tetraethyldisilacyclobutene). Zeitschrift Fur Naturforschung - Section B Journal of Chemical Sciences, 2016, 71, 227-230.	0.3	1
315	Frontispiece: Heterometallic Fe ^{III} /K Coordination Polymer with a Wide Thermal Hysteretic Spin Transition at Room Temperature. Chemistry - A European Journal, 2016, 22, .	1.7	1
316	Isolation and phototransformation of enantiomerically pure iridium(iii) bis[(4,6-difluorophenyl)pyridinato-N,C2]picolinate. RSC Advances, 2017, 7, 29550-29553.	1.7	1
317	Mechanistic Insights into Methane Oxidation by Molecular Oxygen under Photoirradiation: Controlled Radical Chain Reactions. Bulletin of the Chemical Society of Japan, 2019, 92, 1840-1846.	2.0	1
318	Redox properties of a bipyrimidine-bridged dinuclear ruthenium(II) complex. Inorganic Chemistry Communication, 2020, 120, 108150.	1.8	1
319	Mechanistic Understanding of Methane Hydroxylation by Cu-Exchanged Zeolites. , 2020, , 75-86.		1
320	Theoretical Views on Catalytic Reaction Pathways for Nitrogen Fixation by Dinitrogen-Bridging Dimolybdenum Complexes. Yuki Gosei Kagaku Kyokaishi/Journal of Synthetic Organic Chemistry, 2021, 79, 1041-1049.	0.0	1
321	Mechanistic study on reduction of nitric oxide to nitrous oxide using a dicopper complex. Dalton Transactions, 2022, 51, 5399-5403.	1.6	1
322	Synthesis, redox properties, and catalytic hydrogen gas generation of porphycene cobalt complexes. Journal of Porphyrins and Phthalocyanines, 2022, 26, 263-272.	0.4	1
323	Heterointerface Created on Auâ€Clusterâ€Loaded Unilamellar Hydroxide Electrocatalysts as a Highly Active Site for the Oxygen Evolution Reaction (Adv. Mater. 16/2022). Advanced Materials, 2022, 34, .	11.1	1
324	Homogeneous catalyst modifier for alkyne semi-hydrogenation: systematic screening in an automated flow reactor and computational study on mechanisms. Reaction Chemistry and Engineering, 0, , .	1.9	1

#	Article	IF	CITATIONS
325	Frontispiece: Formation and High Reactivity of the <i>anti</i> â€Dioxo Form of Highâ€Spin μâ€Oxodioxodiiron(IV) as the Active Species That Cleaves Strong Câ^'H Bonds. Chemistry - A European Journal, 2016, 22, .	1.7	0
326	Esterification of Tertiary Amides by Alcohols Through Câ^'N Bond Cleavage over CeO 2. ChemCatChem, 2019, 11, 15-15.	1.8	0
327	Theoretical Study on the Relation between the Frontier Orbital and the Conductance in Aromatic Single-Molecular Parallel Circuits. Journal of Computer Chemistry Japan, 2019, 18, 227-229.	0.0	0
328	Theoretical Study of Methanol Oxidation by Ni-ZSM-5. Journal of Computer Chemistry Japan, 2020, 19, 151-153.	0.0	0
329	Theoretical Suggestion of a Methane Hydroxylation Catalyst. Journal of Computer Chemistry Japan, 2020, 19, 133-135.	0.0	0
330	Orbital Concept for Methane Activation. , 2020, , 1-22.		0
331	Augmented Selfâ€Association by Electrostatic Forces in Thienopyrroleâ€Fused Thiadiazoles that Contain an Ester instead of an Ether Linker. Chemistry - an Asian Journal, 2022, 17, .	1.7	0